ISSN: 2688-8645

Failure Model of Nonlinear Creep Damage Evolution of Rock based on PFC

Cheng Xu*

University of Shanghai for Science and Technology, Shanghai 200093, China

*Corresponding Author

Abstract

This study investigates the creep behavior and crack evolution characteristics of rock under axial pressure and shear loads using the Particle Flow Code (PFC2D) software. The results show that the rock exhibits typical three-stage creep behavior, including transient creep, steady-state creep, and residual stability stages under both axial pressure and shear load. Under axial pressure, the displacement decay rate is slower, with compression-dominated deformation and significant suppression of crack propagation due to the confining pressure. This delays the occurrence of accelerated creep. In contrast, under shear load, the displacement decay rate is faster, and cracks propagate along the shear direction, forming a distinct shear band with a failure mode combining tensile and shear fractures. Crack propagation under axial pressure primarily consists of localized shear-type microcracks, reflecting the suppressive effect of confining pressure, while shear load induces crack formation along the maximum shear stress direction, transitioning from tensile microcracks to through-going shear cracks over time. These findings suggest that high confining pressure in deep underground environments can effectively inhibit rock creep deformation, but attention must be given to the evolution of microcracks in locally stressed regions.

Keywords

Rock Creep; Two-dimensional Particle Flow Program; Crack Development.

1. Introduction

In recent years, numerical analysis methods have become crucial for analyzing the creep characteristics of rocks. For example, Lockner and Madden [1] utilized finite difference methods based on renormalization group theory to simulate the creep deformation of brittle rocks. Xu et al. [2], considering the heterogeneity of materials and the degradation characteristics based on material mechanical properties, employed the finite element method to study the micromechanisms of creep damage and instability in brittle rocks. Chen and Konietzky [3] conducted numerical simulations of brittle rock creep instability based on subcritical crack growth theory using block-based discrete element software. Tran et al. [4], when investigating dam stability, proposed the rock-ageing model to simulate the creep behavior of the dam body. Subsequently, Wang et al. [5] developed the bond-ageing model, which can simulate creep within the Particle Flow Code (PFC) based on the rock-ageing theory. Potyondy [6], using stress corrosion theory, established a parallel bond stress corrosion model in the two-dimensional particle flow program, PFC2D. Building on this, several researchers [7-8] also applied the two-dimensional particle flow program to study the discrete element simulations of rock creep instability.

From the dynamic analysis of the above studies, it is evident that while significant research has been conducted on the creep of various rocks, there is still a need for further exploration of the creep characteristics in rocks, particularly in the unique terrains and landforms found in

ISSN: 2688-8645

domestic regions. A numerical simulation of the creep damage in soft rocks could significantly contribute to advancing the understanding of the micromechanisms and instability processes of mudstone creep in engineering applications.

2. PFC Theory and Creep Model of Particle Flow

2.1. Basic Principles of PFC

The Particle Flow Code (PFC) is a numerical simulation technique based on the Discrete Element Method (DEM). Its core concept involves discretizing the object of study into numerous rigid particle units, with particle interactions and motion evolution described by Newton's laws of motion (translational and rotational equations). The forces acting on each particle are determined by contact forces (normal and tangential forces) and non-contact forces (such as gravity), with contact between particles updated in real-time through dynamic calculations.

The contact model between particles governs the macroscopic mechanical behavior of the system. PFC supports various contact models, such as linear and Hertz-Mindlin, and allows for custom bonded or unbonded connections. The bonded model can simulate the cementing characteristics of materials like rocks and concrete, while the damping model is commonly used to simulate time-dependent effects like creep and viscoelasticity. The contact force is calculated based on force-displacement laws, with particles allowed to undergo finite displacements or even complete separation, enabling the simulation of fracture, large deformation, and other discontinuous issues. Macroscopic mechanical parameters (such as elastic modulus and compressive strength) are calibrated using mesoscopic parameters (like particle stiffness, friction coefficient, and bond strength). This process requires correlating with experimental data or theoretical formulas, for instance, by simulating uniaxial compression to inversely derive the macroscopic stress-strain curve.

PFC uses an explicit time integration method to calculate particle motion, with the time step controlled by particle stiffness and mass to ensure numerical stability. This method is widely applied in geotechnical engineering (slope stability, tunnel support), geomechanics (rock fracture, earthquake simulation), and materials science (particle medium flow), particularly excelling in solving nonlinear and damage evolution problems that traditional continuous medium methods struggle to handle.

2.2. Creep Model

Creep models are theoretical frameworks used to study the time-dependent deformation of materials under constant stress, describing the long-term mechanical behavior of materials. Common creep models include linear creep models, power-law creep models, and nonlinear creep models. The linear creep model assumes that the creep rate is proportional to the applied stress, making it suitable for small deformations and low-stress conditions. The power-law creep model is applicable to high-temperature or high-stress environments, where the creep rate follows a power-law relationship with stress. The nonlinear creep model, on the other hand, accounts for the complex characteristics of materials, dividing creep into instantaneous elastic strain, delayed strain, and steady-state creep strain. Additionally, the generalized Maxwell model, which combines springs and dampers, is capable of describing creep behavior over different time scales. These models are of significant importance in engineering design, helping to predict the long-term performance of materials and optimize structural lifespan and safety.

3. Numerical Simulation and Parameter Analysis

The calibration of the model's transient mesoscopic parameters is typically based on the macroscopic mechanical parameters observed in laboratory direct shear tests on rock specimens, such as peak stress, elastic modulus, and Poisson's ratio. These macroscopic

ISSN: 2688-8645

parameters serve as calibration references. By constructing a PFC numerical model, the mesoscopic parameters of particles and their contacts are adjusted to ensure that the macroscopic mechanical properties of the numerical model match the mechanical parameters of the rock specimens from the laboratory tests.

In PFC2D (Particle Flow Code), the fundamental models include the contact model, sliding model, and contact bond model. In typical rock material testing simulations, the contact model and contact bond model are often used to represent the stiffness of rock particles and the cementing agents between particles. However, these models are insufficient for describing the rheological properties of rocks, which is why a rheology model is selected. In this study, the PBM (Parallel Bond Model) rheology model provided by PFC is used, with its basic principles shown in Figure 1. In the figure, $\overline{\sigma}_c$, $\overline{c}$ and $\overline{\varphi}$ represent the viscosity coefficients of the damping units, while K_n , $\overline{K}_n$, K_s and $\overline{K}_s$ are the stiffness coefficients of the spring units. Considering the stiffness characteristics of rock particles, a linear contact model from the contact model is also used concurrently.

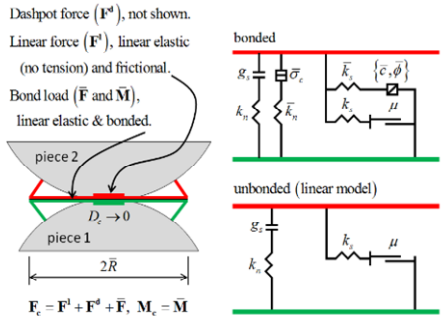

Figure 1. Diagram of bonding between particles

The linear parallel bond model exhibits two types of interfaces: one is infinitesimally small, linear elastic (without tensile forces), and frictional, capable of bearing force; the other is of finite size, linear elastic, and has a bonding effect, capable of bearing both force and moment (as shown in Figure 1). The first type of interface is equivalent to a linear model: it does not resist relative rotation and adapts to sliding by applying a Coulomb limit to the shear force. The second type of interface is referred to as a parallel bond, as it acts in parallel with the first type when in a bonded state. When the second type of interface is bonded, it resists relative rotation, and its properties are linear elastic until the strength limit is reached and the bond breaks (transforming it into an unbonded state). When the second type of interface is in an unbonded state, it does not carry any load. The unbonded linear parallel bond model is equivalent to the linear model.

In the parallel bond model, to represent the bonding strength characteristics, parameters such as the parallel bond tensile strength, parallel bond cohesion, and parallel bond internal friction angle are introduced. The shear strength of the bond is determined using the following Mohr-Coulomb equation:

$$\overline{\tau}_c = \overline{c} - \overline{\sigma} \tan \overline{\varphi} \tag{1}$$

$$\overline{\sigma} = \overline{F}_n / \overline{A} \tag{2}$$

The failure criterion is as follows:

$$\overline{\sigma} \geq \overline{\sigma}_c \rightarrow \text{Tensile failure} \tag{3}$$

$$\overline{\tau} \geq \overline{\tau}_c \rightarrow \text{Shear failure} \tag{4}$$

ISSN: 2688-8645

In the equation: $\bar{\tau}$ represents the bond shear strength; $\bar{c}$ represents the parallel bond cohesion; $\bar{\sigma}$ represents the normal stress; $\bar{\varphi}$ represents the parallel bond internal friction angle; $\bar{F}_n$ represents the normal force; $\bar{A}$ represents the contact area; $\bar{\sigma}_c$ represents the parallel bond tensile strength; and $\bar{\tau}$ represents the shear stress.

That is, when $\bar{\sigma} \geq \bar{\sigma}_c$, the bond behaves as tensile failure, and when $\bar{\tau} \geq \bar{\tau}_c$, the bond behaves as shear failure. Therefore, when the stress at the contact point exceeds the bond strength, bond failure occurs, leading to the failure of the connection between particles, and the model degenerates into a linear model.

When the interface of a planar contact resists torque, its strain energy, as shown in Equation (1), is stored in the connection between individual particles. The contact forces between particles near the planar contact surface are updated in real-time according to the relevant updating rules of the planar mechanical model.

$$\bar{E}_k = \frac{1}{2}\left(\frac{\bar{F}_n^{\,2}}{\bar{k}_n A} + \frac{\left\|\bar{F}_s\right\|^2}{\bar{k}_s \bar{A}} + \frac{\bar{M}_t^{\,2}}{\bar{k}_s \bar{J}} + \frac{\left\|\bar{M}_b\right\|^2}{\bar{k}_n \bar{I}} \right) \tag{5}$$

In the equation, $\bar{E}_k$ represents the strain energy; $\bar{F}_n$ and $\bar{F}_s$ represent the normal and tangential forces, respectively; $\bar{k}_n$ and $\bar{k}_s$ represent the normal and tangential strengths, respectively; $\bar{M}_t$ and $\bar{M}_b$ represent the normal and tangential moments, respectively; $\bar{I}$ and $\bar{J}$ represent the moment of inertia and polar moment of inertia at the contact point, respectively; A represents the contact area of the parallel bond (in PFC2D, the contact area is $2\bar{R}t$, while in PFC3D, the contact area is $\pi\bar{R}^2$).

3.1. Establishment of Numerical Model of Creep Shear Test

Based on the results of the rock sample laboratory tests, the model dimensions are set to the same size as the laboratory samples, 500mm × 500mm (length × height). The sample density is 2700 kg/m^3, and a total of 15,008 particles of different sizes are generated, which includes 21,900 contacts. The minimum particle radius is 2.0 mm, and the maximum particle radius is 2.5 mm.

3.2. Correction and Verification of Transient Mesoscopic Parameters of the Model

Before conducting the simulation, the required mesoscopic parameters for the model are first determined. The key mechanical and contact relationship parameters that influence the parallel bond model include: particle contact modulus , parallel bond modulus , particle stiffness ratio , parallel bond stiffness ratio , parallel bond normal strength, and parallel bond tangential strength , among others. The parameter calibration is performed through the following steps: First, the particle contact modulus and parallel bond modulus are adjusted to match the elastic modulus observed in the laboratory tests. Next, the stiffness ratios are modified to obtain a failure mode similar to that in the laboratory tests. Finally, the parallel bond normal and tangential strengths are adjusted to achieve the peak strength. Based on the sensitivity analysis of the parallel bond model parameters and through iterative calibration using the "trial and error" method, the final PFC mesoscopic parameters that reflect the results of the mudstone laboratory tests are obtained, as shown in Table 1.

ISSN: 2688-8645

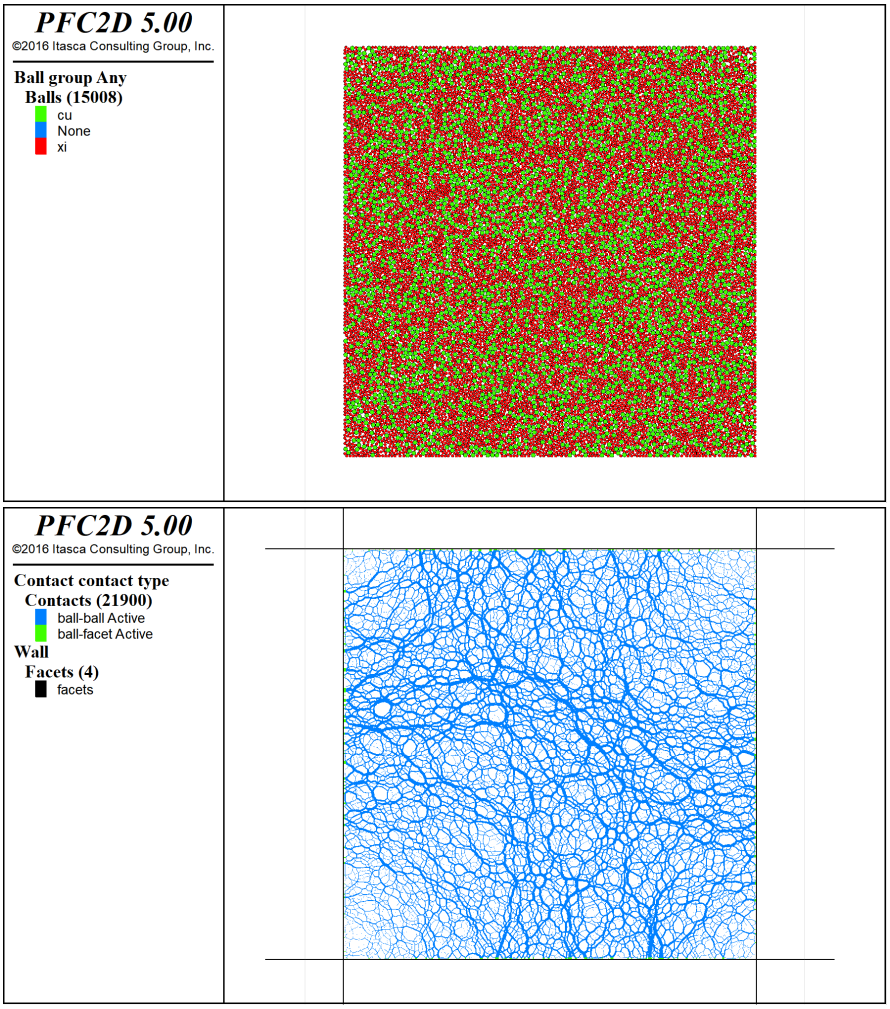

Figure 2. Establishment of particles and contacts

Table 1. Model parameter table

Parameter/unit	Numerical value
Minimum radius of particle /mm	2.0
Maximum radius of particle /mm	3.0
Particle radius ratio	1.5
Elastic modulus of particles /GPa	0.8
Particle stiffness ratio	0.8
Particle friction coefficient	0.5
Wall friction coefficient	0
Average bond contact tensile strength /MPa	5
Average tangential strength of adhesive contact /MPa	8

In Figure 3, when a tangential force of 500 kPa is applied to the side, the ball displacement magnitude (Ball displacement_mag) gradually decays from the initial value of 2.0400×10−22.0400 \times 10^{-2}2.0400×10−2 to zero, indicating that the rock undergoes significant creep deformation under shear load. This can be divided into three distinct stages:

1. Transient Creep Stage (t0 → t1): The displacement magnitude rapidly decreases from 2.04×10^{-2} to 2.04×10^{-2}, corresponding to the rapid initiation and local adjustment of microcracks within the rock. The energy is primarily released as elastic strain energy.
2. Steady-State Creep Stage (t1 → t2): The displacement rate significantly decreases from 1.2×10^{-2} to 4.0×10^{-3}, reflecting that the rock enters a stable deformation phase dominated

ISSN: 2688-8645

by viscous flow, with crack propagation rate and material self-healing effects reaching a dynamic equilibrium.

3. Residual Stability Stage (t2 → t_{end}): The displacement magnitude approaches zero (<4.0×10^{-3}), indicating that the system has reached a new mechanical equilibrium, although caution is required regarding potential accelerated creep risks.

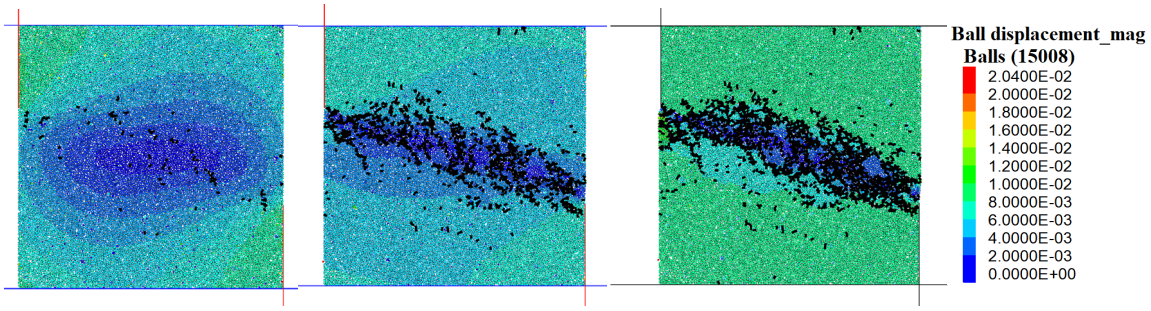

Figure 3. Displacement diagram of tangential stress ball (cracks in black)

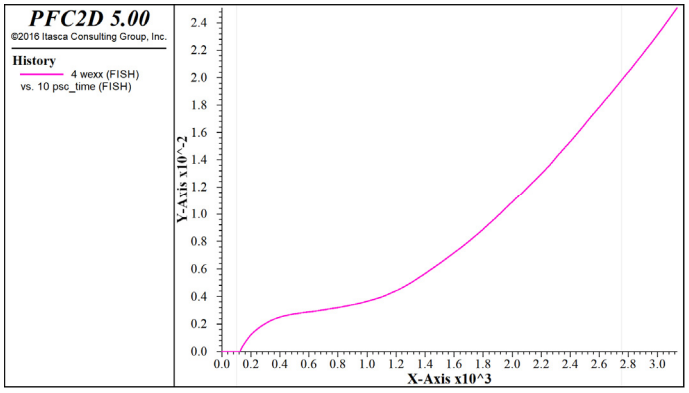

Figure 4. Tangential strain-time diagram

In Figure 5, when an axial pressure of 500 kPa is applied, the ball displacement magnitude (Ball displacement_mag) gradually decays from an initial value of 1.1496×10^{-2} to zero, showing a similar displacement trend as under shear load but with a generally lower displacement magnitude, indicating that the deformation rate of the rock under axial pressure is relatively slower.

1. Transient Creep Stage (t0 → t1): The displacement magnitude rapidly decreases from 2.04×10^{-2} to 1.2×10^{-2}, corresponding to the rapid initiation and local adjustment of microcracks within the rock. The energy is primarily released as elastic strain energy.
2. Steady-State Creep Stage (t1 → t2): The displacement rate significantly decreases from 1.2×10^{-2} to 4.0×10^{-3}, reflecting that the rock enters a stable deformation phase dominated by viscous flow, with crack propagation rate and material self-healing effects reaching a dynamic equilibrium.
3. Residual Stability Stage (t2 → tend): The displacement magnitude approaches zero (<4.0×10^{-3}), indicating that the system has reached a new mechanical equilibrium, although caution is required regarding potential accelerated creep risks.

4. Conclusion

Through the analysis of the creep behavior and crack evolution characteristics of rock under axial pressure and shear loads simulated by PFC2D software, the following main conclusions are drawn:

ISSN: 2688-8645

The rock exhibits typical three-stage creep behavior under both axial pressure and shear load, including the transient creep, steady-state creep, and residual stability stages. Under axial pressure, the displacement decay rate is slower, and the overall deformation is dominated by compression. The confining pressure significantly suppresses crack propagation, delaying the onset of accelerated creep. Under shear load, the displacement decay rate is faster, and cracks propagate along the shear direction, forming a distinct through-going shear band. The failure mode is predominantly a combination of tensile and shear failure. Under axial pressure, cracks are mainly localized shear-type microcracks, distributed relatively scattered without forming a significant through-going failure zone, reflecting the confining pressure's suppressive effect on crack propagation. Under shear load, cracks propagate along the direction of maximum shear stress, initially dominated by tensile microcracks, and later gradually form through-going shear cracks, with a more concentrated failure mode.

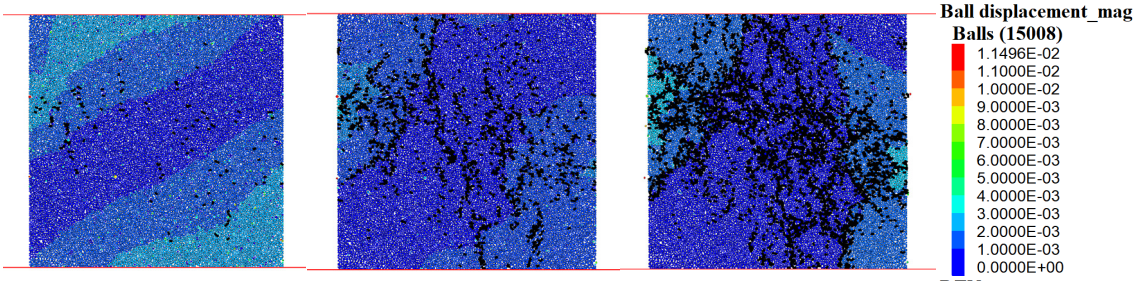

Figure 5. Displacement diagram of axial stress ball (cracks in black)

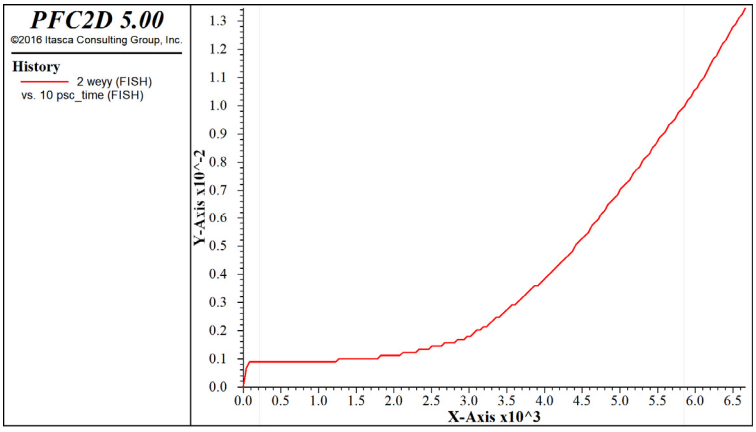

Figure 6. Axial strain-time diagram

In deep underground engineering, a high confining pressure environment can effectively suppress rock creep deformation, but the evolution of microcracks in locally stressed regions still needs attention. It is recommended to use displacement decay rate, axial strain rate, and crack density as key monitoring indicators of creep stability, and combine acoustic emission or microseismic monitoring techniques to assess the degree of rock mass damage in real-time. The numerical model needs further optimization, incorporating anisotropic constitutive relationships and thermo-mechanical-chemical coupling effects, to more accurately simulate rock creep behavior in complex geological environments.

References

[1] Lockner D A, Madden T R. A multiple-crack model of brittle-fracture [J]. Journal of Geophysical Research-Solid Earth, 1991, 96(B12): 19643-19654.

ISSN: 2688-8645

[2] Xu T, Tang C A, Zhao J, et al. Modelling the time-dependent rheological behaviour of heterogeneous brittle rocks [J]. Geophysical Journal International, 2012,189(3): 1781-1796.

[3] Chen W, Konietzky H. Simulation of heterogeneity,creep, damage and lifetime for loaded brittle rocks [J].Tectonophysics, 2014, 633: 164-175.

[4] Tran T H, Vénier R, Cambou B. Discrete modelling of rock-ageing in rockfill dams [J]. Computers and Geotechnics, 2009, 36(1): 264-275.

[5] Wang Y, Zhao Z, Song E. Discrete element modeling of the effect of particle shape on creep behavior of rockfills [J]. International Journal of Environmental, Engineering,2017, 11(9): 803-807.

[6] Potyondy D O. Simulating stress corrosion with a bonded-particle model for rock [J]. International Journal of Rock Mechanics and Mining Sciences, 2007, 44(5):677-691.

[7] Liu Ning, Zhang Chunsheng, Chu Weijiang. Simulating time-dependent failure of deep marble with particle flow code [J]. Chinese Journal of Rock Mechanics and Engineering, 2011, 30(10): 1989-1996.

[8] Sun, J., Chen, M., Jiang, Q., et al. Numerical simulation study on the mesomechanical characteristics of creep damage evolution in Jinping marble. Rock and Soil Mechanics, 2013, 34(12): 3601–3608.